**World Scientific**
www.worldscientific.com

# COMPUTATIONAL STUDY OF BRIDGE-MEDIATED INTERVALENCE ELECTRON TRANSFER. II. COUPLINGS IN DIFFERENT METALLOCENE COMPLEXES

YINXI YU[*], HAOBIN WANG[*,‡] and SHAOWEI CHEN[†,§]

*Department of Chemistry and Biochemistry*
*New Mexico State University, Las Cruces, NM 88003*

†*Department of Chemistry and Biochemistry*
*University of California, Santa Cruz, CA 95064*
‡*haobin@nmsu.edu*
§*shaowei@ucsc.edu*

The constrained density functional theory (CDFT) was used to study bridge-mediated electron transfer processes in mixed-valence systems with two identical metallocene (cobaltocene, ruthenocene, and nickelocene) moieties linked by various bridge structures. Based on the electronic coupling matrix elements obtained from the CDFT calculations, the relationship between the bridge linkage and the effectiveness of intervalence transfer was discussed.

*Keywords*: Intervalence electron transfer; metallocene complexes; constrained density functional theory.

## 1. Introduction

Molecular mixed-valence systems involving metallocene moieties are of tremendous interest in materials science due to the effective electronic communication between different metal centers of the compounds and the resulting unique optoelectronic properties upon photoexcitation.[1−10] According to the traditional classification by Robin and Day,[11] which models the overall system as a donor−bridge−acceptor complex, three types of mixed-valence compounds are identified depending on the degree of charge delocalization or the extent of interactions between the donor and acceptor sites. Class I compounds exhibit little or no donor−acceptor interactions, whereas Class III compounds possess extensive charge delocalization. Class II compounds fall into the intermediate range between I and III. The intervalence electron transfer process in Class II and III complexes is typically ultrafast, exhibiting a characteristic metal-to-metal charge-transfer (MMCT) band in the near-infrared

region. The latter is often used as an optical probe to extract the electronic coupling element $V_{ab}$ (using the Hush formula) between the donor and acceptor states in a mixed-valence compound.

In mixed-valence systems the magnitude of $V_{ab}$ is determined by two contributing factors: (i) direct overlap of the orbitals of the two metal centers (i.e. through-space interactions) and (ii) metal−ligand−metal overlap that may involve $\sigma$ or $\pi$ metal-ligand bonds (i.e. through-bond interactions). When the metal centers are separated by a sufficiently long organic bridge, the contribution from the first factor will be small, whereas the second contribution becomes predominant. Thus, changing the nature of the bridging ligand and/or metal-ligand bonds may have a significant impact on the effective electronic coupling between the two metal centers. This has been observed in previous studies of various donor−bridge−acceptor mixed-valence systems. When two or more identical molecular moieties are linked by a conjugated organic bridge,[8−10,12−24] electronic communication between them is generally very strong. In contrast, when the bridge contains sp[3] carbons, the electronic communication diminishes drastically.[25] With respect to the length of the bridging ligand, a model that is often used to explain the experimental observations is McConnell's superexchange model, in which the effective electronic coupling between the donor and acceptor sites decreases exponentially with the length of the bridge, given that the quantum perturbation theory is valid.

In a previous study,[26] we carried out a computational investigation to examine the bridge-mediated intervalence transfer processes for various ferrocene−bridge−ferrocene model systems. Employing the constrained density functional theory (CDFT), we calculated the electronic coupling elements between the electron donor and acceptor states for these systems, and thus quantified the relationship between the property of the bridge linkage and the electronic communication of the overall system. A practical criterion of classifying the mixed-valence compounds was suggested by gauging the computational results with the experimental observations, where it was found that for compounds with calculated $H_{ab} \sim 1\,\text{kcal/mol}$ in $CH_2Cl_2$ their voltammetric responses were along the borderline of Class I and II complexes in the Robin−Day classification. Based on this result, the intervalence characteristics of unknown compounds could be predicted from the CDFT calculations.

In this paper we extend our computational study of the bridge-mediated intervalence transfer processes to other metallocene-based complexes, i.e. X−bridge−X model systems (X = cobaltocene, ruthenocene, and nickelocene). The motivation of our work is to exploit the electronic properties of other mixed-valence systems and their potential to serve as new functional materials, in addition to ferrocene-based compounds, that possess effective electronic communication among different metal centers. It should be noted that in previous studies the electronic coupling between the metal centers at mixed valence in bicobaltocene derivatives was found to be substantially stronger than that observed with the biferrocene counterparts. This was accounted for by the greater delocalization of the cobalt active orbitals into the ligands and hence a larger donor−acceptor orbital overlap.[27,28] Consequently,

bicobaltocene species generally behave as Class II−III compounds whereas biferro-cene derivatives are mostly Class II. In contrast, the studies of the electronic coupling of binickelocene and biruthenocene derivaties have been relatively scarce.[29−31] Pre-viously, it has been found that binickelocene derivatives exhibited unique anti-ferromagnetic characteritics, suggesting rather extensive intramolecular charge delocalization[30]; whereas studies of the bis(ruthenocenyl) compounds have been largely impeded by the irreversible redox chemistry of the ruthenocene itself.[31] Yet, electrochemical studies of 1,2-bis(ruthenocenyl) ethylene derivatives showed a pair of voltammetric waves that might be ascribed to two one-electron oxidation processes, suggesting a certain degree of ligand-mediated metal−metal interactions between the two ruthenium metal centers.[32,33] Nevertheless, despite substantial efforts in the synthesis and spectroscopic studies of these bimetallocene derivatives, there is a clear lack of quantification of the electronic coupling between the metal centers at mixed valence. It is within this context that this study was conceived and carried out.

In the next section, we will first describe briefly the models and the computational methods employed in this paper. Then we will present the results and detailed analyses on the intervalence coupling/communication. In the conclusion, we will discuss the implication of our computational study in future experimental studies.

## 2. Models and Computational Methods

To study bridge-mediated intervalence electron transfer within different metallocene compounds we consider a model with two metallocene units connected by different organic structural linkages, including saturated C-C single bonds, conjugate C=C double bonds, multiple C≡C triple bonds, aromatic rings, and the mixture between some of them. Unless specified otherwise, the total charge of the initial state for the metallocene−bridge−metallocene compound was set to +1, i.e. an electron will transfer from the donor state ($X^{2+}$) to the acceptor state ($X^{3+}$). In this paper, we mainly considered three metallocene units: cobaltocene, ruthenocene and nick-elocene. Different from ferrocene, the spins of these neutral metallocene compounds are nonzero. We thus took the experimental values, as shown in Table 1, for the neutral compounds and the monocations. Electronic structure calculations have been carried out for various metallocene−bridge−metallocene compounds (neutral and cationic) with other spin multiplicities to verify that these spin states are indeed the ground electronic states for all the compounds considered in this paper.

Table 1.   Spin multiplicity for different metallocene complexes.

| Complex | Neutral compound | Cation (+1 charge) |
|---|---|---|
| Co−bridge−Co | 3 | 2 |
| Ru−bridge−Ru | 1 | 2 |
| Ni−bridge−Ni | 5 | 4 |

Two computational approaches were employed in this work. The standard density functional theory (DFT) was used to optimize the structures and to obtain the equilibrium properties of the mixed-valence complexes. The CDFT[34−40] was used to define (approximately) the donor/acceptor diabatic states and to calculate the electronic coupling matrix element (or transfer integral) for the underlying intervalence transfer.[41] DFT calculations were performed using the quantum chemical programs Gaussian 09,[42] NWCHEM,[43] whereas the CDFT calculations were performed with a modified version of the quantum chemical program NWCHEM. In both simulations, the B3LYP hybrid functional, which includes the Becke three-parameter exchange[44] and the Lee, Yang and Parr correlation functionals,[45] were employed. In most calculations, the SDD basis sets were used in the calculation for the transition metals such as Co, Ni and Ru, whereas the 6-31G** basis sets[46] were used for all other elements such as C, N and H. Using the DFT method, full geometric optimizations were performed in the gas phase for all the systems. When applicable, the solvent effects were taken into account approximately by the COSMO approach.[47]

In the CDFT calculations, an external constraint is imposed via the method of Lagrange multiplier, i.e. an effective potential $V_c w_c(\mathbf{r})$ is added to the Hamiltonian. The resulting ground-state density satisfies specific density constraints, i.e. $\int w_c(\mathbf{r})\rho_c(\mathbf{r})d\mathbf{r} = N_c$, where $w_c(\mathbf{r})$ is the operator that defines the property of interest. For electron transfer processes in transition metal complexes, the constraints can be on both the charges and the spin states. In this work, we employed a simple constraint to define the diabatic states, which is represented by the charge difference ($\Delta q$) between the two metallocene groups: $\Delta q = -1$ for the donor state and $\Delta q = +1$ for the acceptor state. Similar to the standard DFT method, a self-consistent procedure is used to find the minimum energy, the electronic density (or the Kohn−Sham type orbitals), and the constrained potential (the Lagrange multiplier $V_c$) within the CDFT framework. The $2 \times 2$ Hamiltonian matrix is then obtained within the two diabatic basis states.[41] These two states are further orthogonalized via the Löwdin procedure,[48,49] and the electronic coupling matrix element $V_{\mathrm{ab}}$ is just the matrix element $H_{12}$ of the Hamiltonian in the Löwdin basis states.

## 3. Results and Discussion

In our previous study of ferrocene−bridge−ferrocene systems,[26] we have identified three groups of compounds according to the calculated $V_{\mathrm{ab}}$ values in $CH_2Cl_2$ solution. The first group contains the bare diferrocenyl monocation and the compounds with short conjugated bridge structures. The experimental voltammetric measurements for these complexes all exhibit two distinct oxidation processes[22,50,51] in $CH_2Cl_2$. Theoretically, the frontier orbitals of these systems display significant delocalization across the entire complexes, which suggests effective electronic communications between the donor/acceptor states via the superexchange mechanism through the

bridge moieties. The calculated $V_{ab}$ is greater than $1\,kcal/mol$ for these complexes and thus places them as Class II mixed-valence ions.

The second group contains compounds with large aromatic ring bridge units. The calculated $V_{ab}$ is $\sim 1\,kcal/mol$ for these compounds in $CH_2Cl_2$, making them along the borderline between Class I and II compounds in the Robin−Day classification. The relatively weak electronic communication may thus be difficult to resolve experimentally. In fact, in voltammetric measurements one may observe one single pair of broad voltammetric waves or two pairs of overlapping voltammetric peaks.[10] The third group includes bridge units with saturated C−C bonds, for which the calculated $V_{ab}$'s are substantially smaller. Electronic communications between metal centers are fairly weak in these complexes.

For the different metallocene complexes investigated in the present study, the quantification of different groups may be different from those of ferrocene-based compounds. Nevertheless, the calculated $V_{ab}$ is still a good measure of electronic communication. We will thus analyze the results in a similar fashion as in our previous work,[26] and compare our theoretical results with available experimental facts. The calculations were performed with a different solvent, DMF, in which the mixed-valence complexes exhibit slightly stronger electronic communication. The value of electronic coupling that separates Class I and II mixed-valence complexes is thus slightly larger and is estimated to be in the range of $1.0-1.5\,kcal/mol$.

### 3.1. *Simple bridge linkage*

Similar to the ferrocene-based complexes,[26] CDFT calculations are performed to evaluate the electronic coupling elements $V_{ab}$ for the X−bridge−$X^+$ systems, where X = cobaltocene, ruthenocene and nickelocene. The structures for cobaltocene-based complexes are shown in Fig. 1, and those of ruthenocene and nickelocene are similar (and hence not shown). The calculated $V_{ab}$ values (in kcal/mol) are listed in Tables 2−4 for various simple bridge structures. Values in both gas phase and in DMF solution (modeled by the COSMO approach) are listed. The DFT optimized geometries for the neutral complexes were used in all the CDFT calculations. For comparison purpose the results of ferrocene complexes, where new CDFT calculations were performed with the Dimethylformamide (DMF) solvent, are listed in Table 5.

Overall, the three metallocene-based complexes all possess stronger electronic communications than the corresponding ferrocene-based complex with the same bridge structure. This is in qualitative agreement with previous experimental results where the self-exchange rate between cobaltocene and cobaltocenium was found to be more than an order of magnitude greater than that for the respective Fe species.[52−54] Among these, nickelocene-based complexes have the largest electronic coupling elements, followed by the cobaltocene-based and then the ruthenocene-based complexes. Similar to the ferrocene-based complexes, the compounds containing bare dimetallocenyl monocation and those with short conjugated bridge
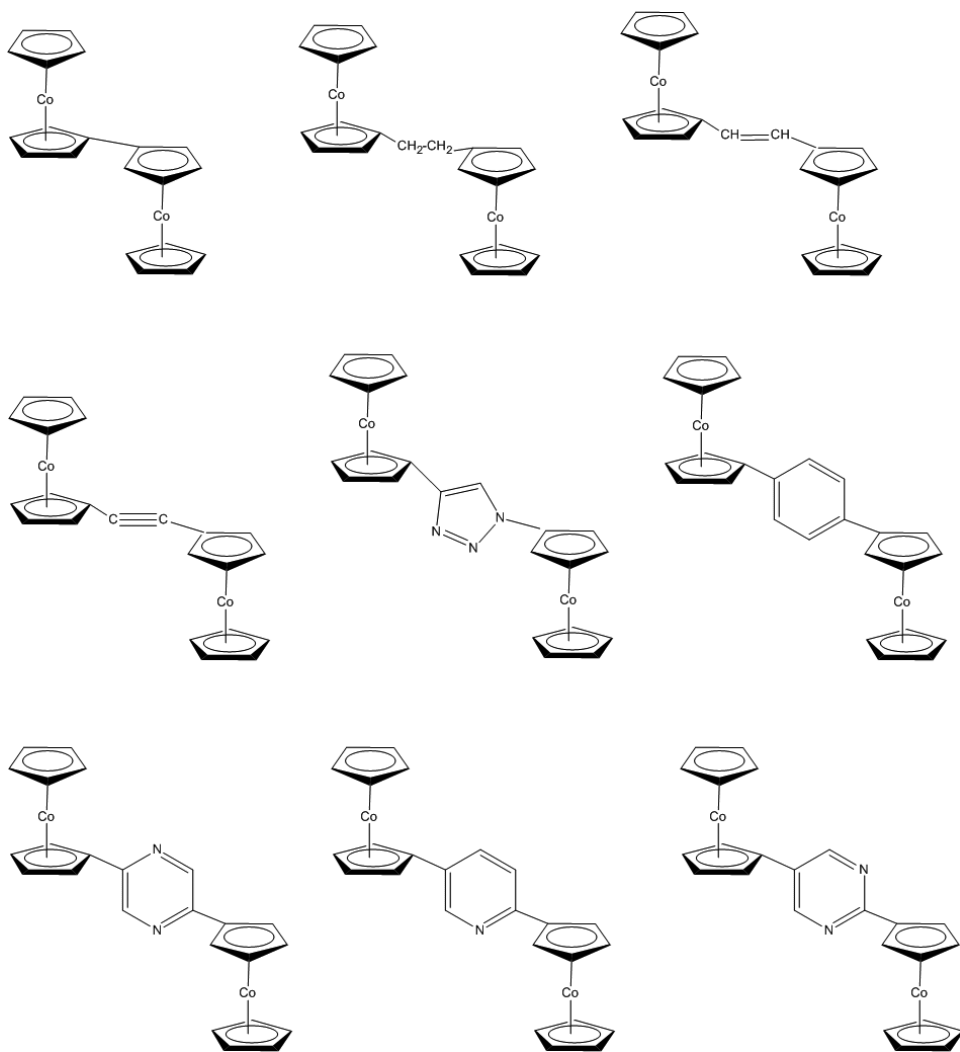
Fig. 1.    Structures of different Co−bridge−Co⁺ systems.

structures such as $-CH=CH-$ and $-C\equiv C-$ all exhibit a $V_{ab}$ value that is markedly greater than $1.5\,kcal/mol$ in DMF solution, indicative of significant intervalence electronic communication and are therefore classified as Class II mixed-valence ions. In experimental measurements, it is likely that these complexes will exhibit two distinguishable voltammetric waves, along with unique near-infrared absorption features.

Differences emerge in the second group of complexes with large aromatic ring bridge units. For ferrocene-based complexes (Table 5), the calculated $V_{ab}$ is in the range of $1-1.5\,kcal/mol$, making them along the borderline between Class I and II compounds according to the Robin−Day classification. The relatively weak electronic

Table 2.   $V_{ab}$ for different $Co-bridge-Co^+$ systems.

| Compound | $V_{ab}$ (kcal/mol) | |
|---|---|---|
| | Gas phase | DMF solution |
| $Co-Co^+$ | 6.89 | 5.94 |
| $Co-CH_2-CH_2-Co^+$ | 1.72 | 0.58 |
| $Co-CH=CH-Co^+$ | 7.15 | 3.34 |
| $Co-C\equiv C-Co^+$ | 8.02 | 3.94 |
| $Co-triazole-Co^+$ | 1.91 | 0.44 |
| $Co-benzene-Co^+$ | 4.77 | 2.03 |
| $Co-pyrazine-Co^+$ | 6.10 | 5.39 |
| $Co-pyridine-Co^+$ | 5.23 | 4.03 |
| $Co-pyrimidine-Co^+$ | 5.91 | 4.56 |

Table 3.   $V_{ab}$ for different $Ru-bridge-Ru^+$ systems.

| Compound | $V_{ab}$ (kcal/mol) | |
|---|---|---|
| | Gas phase | DMF solution |
| $Ru-Ru^+$ | 5.93 | 4.88 |
| $Ru-CH_2-CH_2-Ru^+$ | 2.65 | 1.68 |
| $Ru-CH=CH-Ru^+$ | 6.28 | 5.06 |
| $Ru-C\equiv C-Ru^+$ | 5.87 | 4.69 |
| $Ru-triazole-Ru^+$ | 4.33 | 2.85 |
| $Ru-benzene-Ru^+$ | 4.82 | 3.61 |
| $Ru-pyrazine-Ru^+$ | 4.37 | 3.23 |
| $Ru-pyridine-Ru^+$ | 4.30 | 3.17 |
| $Ru-pyrimidine-Ru^+$ | 3.87 | 2.80 |

communication may thus be difficult to resolve experimentally. For instance, in voltammetric measurements one may observe only a single pair of broad voltammetric waves or two pairs of overlapping voltammetric peaks. In contrast, the calculated $V_{ab}$ values are all larger than 1.5 kcal/mol for cobaltocene-, ruthenocene-, and

Table 4.   $V_{ab}$ for different $Ni-bridge-Ni^+$ systems.

| Compound | $V_{ab}$ (kcal/mol) | |
|---|---|---|
| | Gas phase | DMF solution |
| $Ni-Ni^+$ | 21.21 | 18.70 |
| $Ni-CH_2-CH_2-Ni^+$ | 4.32 | 3.14 |
| $Ni-CH=CH-Ni^+$ | 17.70 | 14.99 |
| $Ni-C\equiv C-Ni^+$ | 16.50 | 13.87 |
| $Ni-triazole-Ni^+$ | 10.66 | 8.47 |
| $Ni-benzene-Ni^+$ | 7.66 | 5.72 |
| $Ni-pyrazine-Ni^+$ | 10.86 | 8.60 |
| $Ni-pyridine-Ni^+$ | 11.36 | 8.97 |
| $Ni-pyrimidine-Ni^+$ | 10.60 | 8.28 |

Table 5.    $V_{ab}$ for different Fc−bridge−Fc$^+$ systems.

| Compound | $V_{ab}$ (kcal/mol) | |
| --- | --- | --- |
|  | Gas phase | DMF solution |
| Fc−Fc$^+$ | 3.26 | 2.20 |
| Fc−CH$_2$−CH$_2$−Fc$^+$ | 0.79 | 0.58 |
| Fc−CH=CH−Fc$^+$ | 3.22 | 2.30 |
| Fc−C≡C−Fc$^+$ | 2.82 | 2.27 |
| Fc−triazole−Fc$^+$ | 1.82 | 1.16 |
| Fc−benzene−Fc$^+$ | 1.99 | 1.43 |
| Fc−pyrazine−Fc$^+$ | 1.78 | 1.35 |
| Fc−pyridine−Fc$^+$ | 1.85 | 1.41 |
| Fc−pyrimidine−Fc$^+$ | 1.69 | 1.27 |

nickelocene-based complexes with the same aromatic ring bridge structures. Based on our CDFT results, these complexes belong to Class II in Robin−Day classification. One indication of the strong electronic communication across the system is the delocalized nature of the frontier orbitals in these compounds, as shown in Fig. 2.

For compounds X−CH$_2$−CH$_2$−X$^+$ and X−triazole−X$^+$, the calculated $V_{ab}$'s display more complex behaviors than for the previously studied ferrocene-based complexes.[26] When X = cobaltocene, the calculated $V_{ab}$'s are substantially smaller than those with the other bridge units listed in the same table. Thus, it is highly likely that these two compounds belong to Class I in Robin−Day classification.
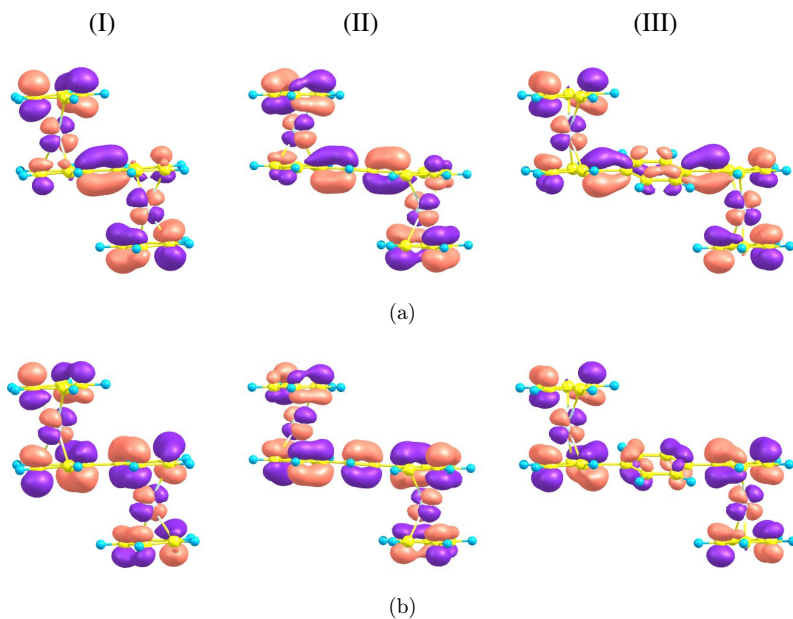
(I)              (II)              (III)



(a)



(b)

Fig. 2.    (a) HOMO and (b) LUMO topological diagrams for (I) Co−Co$^+$, (II) Co−CH=CH-Co$^+$, (III) Co−benzene−Co$^+$.

Table 6. Length dependence of $V_{ab}$ for different Co−bridge−Co$^+$ systems.

| Co−bridge−Co$^+$ | $V_{ab}$ (kcal/mol) | |
|---|---|---|
| | Gas phase | DMF solution |
| (C−C)$_n$ | | |
| Co−CH$_2$−CH$_2$−Co$^+$ | 1.72 | 0.58 |
| Co−(CH$_2$−CH$_2$)$_3$−Co$^+$ | 0.94 | 0.29 |
| Co−(CH$_2$−CH$_2$)$_6$−Co$^+$ | 4.14 | 0.0006 |
| (C=C)$_n$ | | |
| Co−CH=CH−Co$^+$ | 7.15 | 3.34 |
| Co−(CH=CH)$_3$−Co$^+$ | 6.46 | 4.62 |
| Co−(CH=CH)$_6$−Co$^+$ | 4.88 | 2.94 |
| (C≡C)$_n$ | | |
| Co− C≡C−Co$^+$ | 8.02 | 3.94 |
| Co−(C≡C)$_3$−Co$^+$ | 3.19 | 2.28 |
| Co−(C≡C)$_6$−Co$^+$ | 3.45 | 2.16 |

When X = ruthenocene, or nickelocene, both X−CH$_2$−CH$_2$−X$^+$ and X−triazole−X$^+$ have larger $V_{ab}$'s, ranking them at the borderline of Class I and II or Class II mixed-valence complexes.

## 3.2. *Dependence on the bridge length*

Similar to the previous work,[26] CDFT has also been performed to examine the impact of the bridge length on the electronic coupling between the metal centers by using three model systems: (a) X−(CH$_2$−CH$_2$)$_n$−X$^+$, (b) X−(CH=CH)$_n$−X$^+$, (c) X−(C≡C)$_n$−X$^+$, where $n$ is the number of the repetitive bridge structural units. The calculated $V_{ab}$'s are listed in Tables 6−8. For comparison purpose, the results for ferrocene-based complexes are listed in Table 9. These $V_{ab}$ values in general decrease with increasing bridge length ($n$), which is consistent with the common qualitative behavior for long-range electron transfer. In addition, there are some fluctuations in the length dependence of $V_{ab}$. Besides the numerical uncertainties inherent in the CDFT calculations (especially for the gas phase values in Table 6), the deviation from the exponential decay law in the superexchange model could be rationalized by the following reasons as discussed in our previous work.[26] First, the derivation of McConnell's superexchange theory is based on the quantum perturbation theory, which may not be valid for intervalence transfer where strong electronic coupling is present. Second, McConnell's model assumes identical bridge energy levels. If there is some disorder in the bridge, it will disrupt the exponential decay. Third, if there is true delocalization across the bridge, then the coupling does not have to decay at all. In general, the calculated electronic coupling elements are quite large for conjugate bridge structures even when $n$ is large, suggesting effective electronic communication over a long distance.

Table 7. Length dependence of $V_{ab}$ for different Ru−bridge−Ru$^+$ systems.

| Ru−bridge−Ru$^+$ | $V_{ab}$ (kcal/mol) | |
|---|---|---|
| | Gas phase | DMF solution |
| $(C-C)_n$ | | |
| Ru−CH$_2$−CH$_2$−Ru$^+$ | 2.65 | 1.68 |
| Ru−(CH$_2$−CH$_2$)$_3$−Ru$^+$ | 5.80 | 0.53 |
| Ru−(CH$_2$−CH$_2$)$_6$−Ru$^+$ | 9.98 | 0.08 |
| $(C=C)_n$ | | |
| Ru−CH$=$CH−Ru$^+$ | 6.28 | 5.06 |
| Ru−(CH$=$CH)$_3$−Ru$^+$ | 8.47 | 6.19 |
| Ru−(CH$=$CH)$_6$−Ru$^+$ | 11.01 | 6.90 |
| $(C\equiv C)_n$ | | |
| Ru−C$\equiv$C−Ru$^+$ | 5.87 | 4.69 |
| Ru−(C$\equiv$C)$_3$−Ru$^+$ | 5.71 | 3.93 |
| Ru−(C$\equiv$C)$_6$−Ru$^+$ | 5.66 | 2.94 |

## 3.3. *Hybrid bridge linkage*

In practice more flexible bridge linkage may be needed for the purpose of designing effective synthetic routes or enhancing certain physical/chemical properties of the overall mixed-valence complex. In these situations, a hybrid bridge linkage may be a more preferable choice. Table 10 summarizes the results with varied hybrid (conjugated) bridge linkages. As we can see, all the compounds exhibit large electronic couplings, which may be due to the effective conjugation in the bridge structure and a fairly short length of the bridge. Furthermore, −C$\equiv$C− spacers apppear to be more effective in facilitating donor−acceptor electronic interactions than the phenyl moieties.

Table 8. Length dependence of $V_{ab}$ for different Ni−bridge−Ni$^+$ systems.

| Ni−bridge−Ni$^+$ | $V_{ab}$ (kcal/mol) | |
|---|---|---|
| | Gas phase | DMF solution |
| $(C-C)_n$ | | |
| Ni−CH$_2$−CH$_2$−Ni$^+$ | 4.32 | 3.14 |
| Ni−(CH$_2$−CH$_2$)$_3$−Ni$^+$ | 5.40 | 1.10 |
| Ni−(CH$_2$−CH$_2$)$_6$−Ni$^+$ | 9.29 | 0.09 |
| $(C=C)_n$ | | |
| Ni−CH$=$CH−Ni$^+$ | 17.70 | 14.99 |
| Ni−(CH$=$CH)$_3$−Ni$^+$ | 16.19 | 12.30 |
| Ni−(CH$=$CH)$_6$−Ni$^+$ | 14.75 | 9.45 |
| $(C\equiv C)_n$ | | |
| Ni−C$\equiv$C−Ni$^+$ | 16.50 | 13.87 |
| Ni−(C$\equiv$C)$_3$−Ni$^+$ | 3.71 | 2.72 |
| Ni−(C$\equiv$C)$_6$−Ni$^+$ | 8.97 | 5.49 |

Table 9. Length dependence of $V_{ab}$ for different Fc−bridge−Fc$^+$ systems.

| Fc−bridge−Fc$^+$ | $V_{ab}$ (kcal/mol) | |
|---|---|---|
| | Gas phase | DMF solution |
| (C−C)$_n$ | | |
| Fc−CH$_2$−CH$_2$−Fc$^+$ | 0.79 | 0.58 |
| Fc−(CH$_2$−CH$_2$)$_3$−Fc$^+$ | 0.15 | 0.07 |
| Fc−(CH$_2$−CH$_2$)$_6$−Fc$^+$ | 0.03 | 0.004 |
| (C=C)$_n$ | | |
| Fc−CH=CH−Fc$^+$ | 3.22 | 2.30 |
| Fc−(CH=CH)$_3$−Fc$^+$ | 3.42 | 2.53 |
| Fc−(CH=CH)$_6$−Fc$^+$ | 1.02 | 0.05 |
| (C≡C)$_n$ | | |
| Fc−C≡C−Fc$^+$ | 2.82 | 2.27 |
| Fc−(C≡C)$_3$−Fc$^+$ | 2.00 | 1.42 |
| Fc−(C≡C)$_6$−Fc$^+$ | 1.39 | 0.81 |

## 3.4. *Comparison with* $V_{ab}$ *values obtained from approximate approaches*

As pointed out in our previous paper,[26] there are a few approximate ways of estimating the electronic coupling elements from the DFT or CDFT energies. Yet they yielded inaccurate results for the ferrocene systems due to the self-interaction error present in the approximate density functional.[41] Here we perform the same analysis for the metallocene systems studied in this paper. The first approach employs Koopman's theorem,[55,56] where the value of $V_{ab}$ is simply approximated as one-half of the energy gap between the highest occupied molecular orbital (HOMO) and the lowest unoccupied molecular orbital (LUMO). The second approach extracts the value of $V_{ab}$ from the energy differences between the diabatic states obtained from the CDFT calculations and the adiabatic ground-state obtained from the standard

Table 10. $H_{ab}$ for the X−bridge−X systems with hybrid bridge linkage.

| Compound | $H_{ab}$ (kcal/mol) | |
|---|---|---|
| | Gas phase | DMF solution |
| Co−CH=CH−C≡C−CH=CH−Co$^+$ | 6.16 | 4.42 |
| Co−CH=CH−benzene−CH=CH−Co$^+$ | 4.09 | 2.63 |
| Ru−CH=CH−C≡C−CH=CH−Ru$^+$ | 7.74 | 5.49 |
| Ru−CH=CH−benzene−CH=CH−Ru$^+$ | 6.71 | 4.28 |
| Ni−CH=CH−C≡C−CH=CH−Ni$^+$ | 14.81 | 11.17 |
| Ni−CH=CH−benzene−CH=CH−Ni$^+$ | 11.42 | 7.78 |
| Fc−CH=CH−C≡C−CH=CH−Fc$^+$ | 2.87 | 2.08 |
| Fc−CH=CH−benzene−CH=CH−Fc$^+$ | 2.11 | 1.78 |

Table 11.   Comparison of $V_{ab}$ values obtained from the HOMO−LUMO Gap, Eq. (1), and the CDFT calculation for the Co−bridge−Co systems.

| Compound | $V_{ab}$ from HOMO−LUMO gap | $V_{ab}$ from Eq. (1) | $V_{ab}$ from CDFT |
|---|---|---|---|
| Co−Co$^+$ | 15.69 | 11.48 | 6.89 |
| Co−CH$_2$−CH$_2$−Co$^+$ | 5.81 | 8.99 | 1.72 |
| Co−CH=CH−Co$^+$ | 13.74 | 15.56 | 7.15 |
| Co−C≡C−Co$^+$ | 13.52 | 15.83 | 8.02 |
| Co−triazole−Co$^+$ | 6.59 | 11.06 | 1.91 |
| Co−benzene−Co$^+$ | 9.29 | 13.33 | 4.77 |
| Co−pyrazine−Co$^+$ | 10.57 | 14.45 | 6.10 |
| Co−pyridine−Co$^+$ | 9.73 | 13.58 | 5.23 |
| Co−pyrimidine−Co$^+$ | 10.32 | 14.06 | 5.91 |
| Co−(CH$_2$−CH$_2$)$_3$−Co$^+$ | 2.89 | 10.35 | 0.94 |
| Co−(CH$_2$−CH$_2$)$_6$−Co$^+$ | 1.60 | 12.71 | 4.14 |
| Co−(CH=CH)$_3$−Co$^+$ | 10.98 | 17.36 | 6.46 |
| Co−(CH=CH)$_6$−Co$^+$ | 8.31 | 18.20 | 4.88 |
| Co−(C≡C)$_3$−Co$^+$ | 7.37 | 14.26 | 3.19 |
| Co−(C≡C)$_6$−Co$^+$ | 6.21 | 16.03 | 3.45 |
| Co−CH=CH−C≡C−CH=CH−Co$^+$ | 10.48 | 16.88 | 6.16 |
| Co−CH=CH−benzene−CH=CH−Co$^+$ | 7.50 | 15.21 | 4.09 |

unconstrained DFT calculations

$$|H_{ab}| = \frac{\sqrt{(E - E_D)(E - E_A)} - S\frac{(E-E_D)+(E-E_A)}{2}}{1 - S^2}, \tag{1}$$

where $E_D$ and $E_A$ are the diabatic state energies for the donor and acceptor, respectively, $S$ is the overlap between the two diabatic states, and $E$ represents the ground-state energy obtained from the unconstrained DFT.

The $V_{ab}$'s obtained using the above two approaches, as listed in Table 11, are much larger than those obtained directly from the CDFT calculation. This is similar to the previous study of ferrocene-based mixed-valence systems,[26] and may be attributed to the self-interaction errors for systems with fractional charges, which severely underestimates the DFT energy. Therefore, it is preferable to avoid using the DFT results to calculate the coupling element. Upon closer examination the adiabatic energy curve generated from the DFT calculation is well below the CDFT-generated diabatic energy curves along the whole reaction coordinate, which is unphysical and signals the self-interaction error. This may be corrected, using the CDFT energies, by shifting the adiabatic curve up according to the reference where the coupling is zero. In this way the self-interaction error has been reduced and the electronic coupling obtained from Eq. (1) would be more accurate.

### 3.5. Sensitivity of $V_{ab}$ to the variation of nuclear geometries

The charge-localized states obtained from the CDFT simulation represents approximate diabatic states, within which the electronic coupling $V_{ab}$ should vary

relatively slowly with respect to the change in nuclear configurations. The commonly used Condon approximation in electron transfer theory treats $V_{ab}$ as a constant. Following our previous work,[26] we investigate the validity of the Condon approximation in the regime most relevant to the electron transfer process: from the minima of the diabatic states to the crossing point, as well as nuclear geometries whose energies are reasonably close to these important configurations (e.g. within several kcal/mol). Specifically, we consider the following representative examples of a few X−bridge−X systems: (1) the unoptimized geometries with energies several kcal/mol higher than those of the optimized geometries; (2) the optimized geometries from the standard unconstrained DFT calculation and (3) the optimized charge-localized geometries obtained from the CDFT calculations, which were obtained by invoking the constraint that one metallocene group has one more electron than the other and performing the geometry optimization under this constraint. Table 12 lists the corresponding gas-phase and solution-phase $V_{ab}$ values for several representative molecules at different geometries. It is obvious that all the $V_{ab}$'s exhibit rather weak

Table 12. Structure dependence of $V_{ab}^{\#}$.

| Compound | Geometry | Relative energy (kcal/mol) | $V_{ab}$(kcal/mol) Gas phase | DMF |
|---|---|---|---|---|
| Co−Co$^+$ | Unoptimized geometry | 1.66 | 13.49 | 11.73 |
| | DFT optimized (no symmetry) | 0 | 6.89 | 5.94 |
| | CDFT optimized | 4.02 | 11.36 | 9.91 |
| Co−CH$_2$−CH$_2$−Co | Unoptimized geometry | 1.57 | 2.65 | 1.98 |
| | DFT optimized (no symmetry) | 0 | 1.72 | 0.58 |
| | CDFT optimized | 0.68 | 2.11 | 1.58 |
| Co−CH=CH−Co$^+$ | Unoptimized geometry | 1.46 | 10.25 | 5.22 |
| | DFT optimized (no symmetry) | 0 | 7.15 | 3.34 |
| | CDFT optimized | 2.22 | 8.96 | 7.34 |
| Ru−Ru$^+$ | Unoptimized geometry | 0.97 | 5.70 | 4.67 |
| | DFT optimized (no symmetry) | 0 | 5.93 | 4.88 |
| | CDFT optimized | 1.86 | 7.47 | 6.22 |
| Ru−CH$_2$−CH$_2$−Ru | Unoptimized geometry | 0.19 | 1.46 | 0.99 |
| | DFT optimized (no symmetry) | 0 | 2.65 | 1.68 |
| | CDFT optimized | 0.57 | 1.16 | 0.78 |
| Ru−CH=CH−Ru$^+$ | Unoptimized geometry | 0.59 | 5.93 | 4.74 |
| | DFT optimized (no symmetry) | 0 | 6.28 | 5.06 |
| | CDFT optimized | 1.25 | 7.53 | 6.09 |
| Ni−Ni$^+$ | Unoptimized geometry | 1.99 | 37.21 | 33.13 |
| | DFT optimized (no symmetry) | 0 | 21.21 | 18.70 |
| | CDFT optimized | 1.31 | 22.03 | 19.52 |
| Ni−CH$_2$−CH$_2$−Ni$^+$ | Unoptimized geometry | 20.71 | 2.27 | 1.59 |
| | DFT optimized (no symmetry) | 0 | 4.32 | 3.14 |
| | CDFT optimized | 0.62 | 4.78 | 3.49 |
| Ni−CH=CH−Ni$^+$ | Unoptimized geometry | 3.5 | 15.97 | 13.55 |
| | DFT optimized (no symmetry) | 0 | 17.70 | 14.99 |
| | CDFT optimized | 0.25 | 16.94 | 14.37 |

$^\#$ For each molecule, the energy of DFT optimized geometry (with C$_1$ symmetry) is set to be the reference.

dependence on the nuclear geometries: the ranges of variation are all within a factor of two. This suggests that the diabatic representation by the CDFT calculations is quite robust. For the purpose of describing the electron transfer reaction and electronic communication between the diabatic states the coupling $V_{ab}$ only needs to be evaluated in a few representative nuclear configurations.

## 4. Conclusion

In this study, the CDFT method was employed to study intervalence transfer in different metallocene−bridge−metallocene model systems. It provided a quantitative description of the intervalence transfer by calculating the electronic coupling between the electron donor and acceptor states. This offered a direct measure of the level of electronic communication at mixed valence. The results showed that the three bimetallocene systems have extremely strong electronic coupling, in comparison with the ferrocene-based species,[26] which may serve as a benchmark for ultrafast electron transfer process and can be used as a reference for the design and interpretation of experiment work.

The metallocene−bridge−metallocene systems considered in this paper all have bigger electronic couplings than the ferrocene systems investigated earlier.[26] This indicates that favorable electric/optical properties may be achieved by considering these metallocene compounds. Despite some difficulties in actual synthesis, our computational work provides some driving force for carrying out more experimental studies on such systems that may eventually pay off.

### References

1. Hush NS, *Coord Chem Rev* **64**:135, 1985.
2. Prassides K, *Mixed Valency Systems: Applications in Chemistry, Physics, and Biology*, Kluwer Academic Publishers, Dordrecht, Boston, 1991.
3. Crutchley RJ, *Adv Inorg Chem* **41**:273, 1994.
4. Astruc D, *Electron Transfer and Radical Processes in Transition-Metal Chemistry*, VCH, New York, NY, 1995.
5. Ward MD, *Chem Soc Rev* **24**:121, 1995.
6. Allen GC, Hush NS, in Cotton, *Progress in Inorganic Chemistry*, FA (ed.), pp. 357−389, 2007.
7. Ceccon A, Santi S, Orian L, Bisello A, *Coord Chem Rev* **248**:683, 2004.

8. Shu P, Bechgaard K, Cowan DO, *J Org Chem* **41**:1849, 1976.
9. Engtrakul C, Sita LR, *Nano Lett* **1**:541, 2001.
10. Low PJ, Roberts RL, Cordiner RL, Hartl F, *J Solid State Electrochem* **9**:717, 2005.
11. Robin MB, Day P, *Adv Inorg Chem Radiochem* **10**:247, 1967.
12. Cowan DO, Levanda C, Park J, Kaufman F, *Acc Chem Res* **6**:1, 1973.
13. Day P, Hush NS, Clark RJH, *Phil Trans Roy Soc Math Phys Eng Sci* **366**:5, 2008.
14. Gamelin DR, Bominaar EL, Mathoniere C, Kirk ML, Wieghardt K, Girerd JJ, Solomon, EI, *Inorg Chem* **35**:4323, 1996.
15. Williams RD, Petrov VI, Lu HP, Hupp JT, *J Phys Chem A* **101**:8070, 1997.
16. Brunschwig BS, Creutz C, Sutin N, *Chem Soc Rev* **31**:168, 2002.
17. Sun H, Steeb J, Kaifer AE, *J Am Chem Soc* **128**:2820, 2006.
18. Concepcion JJ, Dattelbaum DM, Meyer TJ, Rocha RC, *Phil Trans Roy Soc Math Phys Eng Sci* **366**:163, 2008.
19. Osella D, Gobetto R, Nervi C, Ravera M, D'Amato R, Russo MV, *Inorg Chem Commun* **1**:239, 1998.
20. Burgess MR, Jing S, Morley, CP, *J Organomet Chem* **691**:3484, 2006.
21. Wedeking K. Mu ZC, Kehr G, Sierra JC, Lichtenfeld CM, Grimme S, Erker G, Frohlich R, Chi LF, Wang WC, Zhong DY, Fuchs H, *Chem Eur J* **12**:1618, 2006.
22. Ferguson G, Glidewell C, Opromolla G, Zakaria CM, Zanello P, *J Organomet Chem* **517**:183, 1996.
23. Arisandy C, Fullam E, Barlow S, *J Organomet Chem* **691**:3285, 2006.
24. Morrison WH, Krogsrud S, Hendrick DN, *Inorg Chem* **12**:1998, 1973.
25. Nishihara H, *Bull Chem Soc Jpn* **74**:19, 2001.
26. Ding FZ, Wang HB, Wu Q, Van Voorhis T, Chen SW, Konopelski JP, *J Phys Chem A* **114**:6039, 2010.
27. Mcmanis GE, Nielson RM, Weaver MJ, *Inorg Chem* **27**:1827, 1988.
28. Jones SC, Barlow S, O'Hare D, *Chem Eur J* **11**:4473, 2005.
29. Smart JC, Pinsky BL, *J Am Chem Soc* **99**:956, 1977.
30. Hilbig H, Hudeczek P, Kohler FH, Xie XL, Bergerat P, Kahn O, *Inorg Chem* **37**:4246, 1998.
31. Barlow S, Marder SR, *Chem Commun* 1555, 2000.
32. Sato M, Kudo A, Kawata Y, Saitoh H, *Chem Commun* 25, 1996.
33. Sato M, Kawata Y, Kudo A, Iwai A, Saitoh H, Ochiai S, *J Chem Soc, Dalton Trans* 2215, 1998.
34. Dederichs PH, Blugel S, Zeller R, Akai H, *Phys Rev Lett* **53**:2512, 1984.
35. Wu Q, Van Voorhis T, *Phys Rev A* **72**:024502, 2005.
36. Wu Q, Van Voorhis T, *J Chem Theory Comput* **2**:765, 2006.
37. Behler J, Delley B, Lorenz S, Reuter K, Scheffler M, *Phys Rev Lett* **94**:036104, 2005.
38. Behler J, Delley B, Reuter K, Scheffler M, *Phys Rev B* **75**:115409, 2007.
39. Schmidt JR, Shenvi N, Tully JC, *J Chem Phys* **129**:114110, 2008.
40. Oberhofer H, Blumberger J, *J Chem Phys* **131**:064101, 2009.
41. Wu Q, Van Voorhis T, *J Chem Phys* **125**:164105, 2006.
42. Frisch MJ *et al.*, Gaussian, Inc., Wallingford, CT, 2004.
43. Bylaska EJ, de Jong WA, Kowalski K, Straatsma, TP, Valiev M, Wang D, Aprà E, Windus TL, Hirata S, Hackler MT, Zhao Y, Fan P-D, Harrison RJ, Dupuis M, Smith DMA, Nieplocha J, Tipparaju V, Krishnan M, Auer AA, Nooijen M, Brown E, Cisneros G, Fann GI, Früchtl H, Garza J, Hirao K, Kendall R, Nichols J, Tsemekhman K, Wolinski K, Anchell J, Bernholdt D, Borowski P, Clark T, Clerc D, Dachsel H, Deegan M, Dyall K, Elwood D, Glendening E, Gutowski M, Hess A, Jaffe J, Johnson B, Ju J, Kobayashi R, Kutteh R, Lin Z, Littlefield R, Long X, Meng B, Nakajima T, Niu S, Rosing

M, Sandrone G, Stave M, Taylor H, Thomas G, van Lenthe J, Wong A, Zhang Z, Pacific Northwest National Laboratory, Richland, Washington 99352-0999, USA, 2006.

44.  Becke AD *J Chem Phys* **98**:5648, 1993.
45.  Lee CT, Yang WT, Parr RG, *Phys Rev B* **37**:785, 1988.
46.  Francl MM, Pietro WJ, Hehre WJ, Binkley JS, Gordon MS, Defrees DJ, Pople JA, *J Chem Phys* **77**:3654, 1982.
47.  Klamt A, Schuurmann G, *J Chem Soc, Perkin Trans* **2**:799, 1993.
48.  Lowdin PO, *J Chem Phys* **18**:365, 1950.
49.  Mayer I, *Int. J. Quant Chem* **90**:63, 2002.
50.  Powers MJ, Meyer TJ, *J Am Chem Soc* **100**:4393, 1978.
51.  Bildstein B, Denifl P, Wurst K, Andre M, Baumgarten M, Friedrich J, Ellmerermuller E, *Organometallics* **14**:4334, 1995.
52.  Nielson RM, Golovin MN, Mcmanis GE, Weaver MJ, *J Am Chem Soc* **110**:1745, 1988.
53.  Nielson RM, Mcmanis GE, Golovin MN, Weaver MJ, *J Phys Chem* **92**:3441, 1988.
54.  Mcmanis GE, Nielson RM, Gochev A, Weaver MJ, *J Am Chem Soc* **111**:5533, 1989.
55.  RodriguezMonge L, Larsson S, *J Phys Chem* **100**:6298, 1996.
56.  Paddon-Row MN, Wong SS, *Chem Phys Lett* **167**:432, 1990.